ELSEVIER

Surface and Coatings Technology 124 (2000) 235–242

SURFACE & COATINGS TECHNOLOGY

www.elsevier.nl/locate/surfcoat

Influence of coating microstructure on the abrasive wear resistance of WC/Co cermet coatings

H. Liao, B. Normand *, C. Coddet

Laboratoire d'Etudes et de Recherches sur les Materiaux et Propriétés de surfaces, IPSé, BP 449, F-90010 Belfort Cedex, France

Received 31 July 1998; accepted in revised form 24 November 1999

Abstract

Thermally sprayed WC/Co cermet coatings are widely used for their resistance to abrasive wear. In this work the influence of the abrasive grain size on the abrasive wear resistance was investigated for WC/Co coatings sprayed with several processes: APS, high-velocity oxy-fuel (HVOF) and VPS. Results show that the larger the abrasive particle size, the lower the abrasion resistance of the coatings. Moreover, among the thermal spray techniques tested, HVOF coatings have the best wear resistance while VPS coatings present the lowest resistance. The role of the coating microstructure and residual stresses on the wear track and morphologies, as well as the abrasive wear behaviour, are discussed. © 2000 Elsevier Science S.A. All rights reserved.

Keywords: Abrasion; Cermet; Thermal spraying; Tungsten carbide; Wear

1. Introduction

Cermet thermal spray coatings are widely used in wear situations because they combine several advantages such as resistance to abrasion, erosion, high temperature and corrosive atmospheres [1]. Numerous works have been devoted to the development of spraying conditions, and characterization of the specific abrasive and erosive wear resistances of the coatings [2].

In the case of two surfaces in relative movement, abrasive wear results from the displacement or removal of material due to the presence of hard particles or hard protuberances in one or both of these two surfaces [3]. Hard particles may come from the material itself or from outside the tribosystem. A protuberance can be considered a hard 'particle' if its surface is harder than that of the counterpart. Generally, the level of abrasive wear depends on the difference between the hardness of the abrasive particle and that of the counter material [3]. So, the high hardness of carbides presents an attractive solution for protecting surfaces against abrasive wear.

On the other hand, the toughness of carbides is limited and, to improve this property, the so-called cermet structure is used. However, the ratio of carbide particles to matrix must be large enough. For sintered specimens, it has been shown that the size, hardness and toughness of the carbide particles control the wear resistance of the material [3]. The same conclusions have been obtained for WC/Co coatings produced by thermal spraying [4,5]; but in this case, the abrasive wear resistance is also related to the spraying conditions [6].

For these coatings, the preferable morphology required for good wear resistance corresponds to well-dispersed fine and hard particles [7]. It appears nowadays that the technique most adapted to reach this type of microstructure by thermal spraying is the high-velocity oxy-fuel (HVOF) process [8], although similar morphologies may be obtained by using other thermal spraying processes. In fact, in order to obtain excellent tribological performance, this morphology must be accompanied by a crystal structure adapted to reach the cohesion of the as-sprayed composite material. This crystal structure, which is described in several papers, is generally attributed to a transformation corresponding to decomposition of the WC particles and/or oxidation of the composite during spraying because of its interaction with air at high temperature [9].

Two steps are generally considered for the material transformations. The first is the decarburization of WC related to the flame temperature and to the dwell time

* Corresponding author. Tel.: +33-3-84-58-31-63; fax: +33-3-84-58-30-30.

E-mail address: bernard.norman@utbm.ft (B. Normand)

PII: S0257-8972(99)00653-2

of the particle in the flame. Nerz et al. proposed the two following reactions [7] for which the higher the temperature, the higher the degree of decarburization:

$$2WC \rightarrow W_2C + C \quad (1)$$

$$W_2C \rightarrow 2W + C. \quad (2)$$

Verdon et al. have described a marked carbon loss in the coating [10] associated with its oxidation in the flame according to the following reaction [7]:

$$2C + O_2 \rightarrow 2CO\ (gas). \quad (3)$$

This oxidation process can be modified both by the oxygen content in the flame [11] and by the air engulfment [12].

The second transformation step is the diffusion of tungsten and carbon liberated according to Eq. (2) into the cobalt matrix. Several authors describe the presence of an amorphous or nanocrystalline supersaturated Co(W,C) solid solution in cermet coatings and also the presence of mixed carbide (η-phase) [7,10,11,13,14]. The presence of free metallic tungsten in the coating was precisely located on the WC crystal surface by Nerz et al. [7] and near the intersplat boundary by Verdon et al. [10]; it was also associated to the carbon loss.

All of these transformations are conditioned by the thermal spraying conditions and diffusion of the elements composing the hard particles in the metallic matrix appears to be the key for coating cohesion and wear resistance. Meanwhile, the properties and performance of tungsten carbide coatings are also related to the carbide size, shape and distribution, as well as to the porosity and the amount of free carbon [15].

The recent development of HVOF spraying devices is largely due to their ability to produce carbide-based coatings with a minimum porosity and decarburization [16–18]. Using the rubber wheel abrasive test, Dorfman et al. [16,19] have observed a lower abrasion resistance for plasma-sprayed coatings compared with HVOF coatings corresponding to a higher decarburization in the former case. Using the same abrasion resistance test, Mäntylä et al. [17] have evaluated WC/Co (12% and 17% cobalt) coatings deposited by VPS, APS, HVOF and DG (detonation gun) processes; results have shown that HVOF and DG give the best properties, the VPS coating containing 17% cobalt presented a relatively weak resistance to abrasion even if its hardness was fairly high. The authors concluded that a uniform and fine carbide particle distribution improves the abrasion resistance. It is now clear that the size and distribution of the hard phase particles are the key factors determining the performance of such coatings; apart from the grain size of the abrasive medium, which has also to be taken into account [3,20].

To extend this knowledge, the aim of this work was to evaluate the influence of the abrasive grain size on the abrasion resistance of typical WC/Co coatings, together with the role of the residual stresses arising from the coating process. In this way, different spray systems and sizes of abrasive particles were used to explore which process is more adapted for different application conditions and cost-effective industrial solutions.

2. Experimental conditions

Coatings were sprayed on to 25CD4 (0.25% carbon, 1% chromium) steel disc substrates of 40 mm diameter and 6 mm thickness. Coatings were deposited using APS, HVOF and VPS following the conditions described in Table 1.

Thermal spray runs were carried out using WC–17% Co commercial agglomerated sintered powders with two different particle-size distributions related to the typical spraying technique; their main characteristics are given in Table 2. The thickness of the coatings was fixed to 300 μm.

Percentages of porosity were determined by image analysis using Optilab® and Image [from the National Institute of Health (NIH), Springfield, VA, USA] softwares. The reported values are the average of 20 measurements made on cross-sections of each coating.

Microhardnesses were measured with a Vickers indentor with a load of 300 g applied during 15 s. The value given is the average of 10 measurements.

Coating morphologies were identified by optical microscopy analyses on specimen cross-sections.

Crystal structures were determined by means of X-ray diffraction (XRD) with Cu Kα ($\lambda = 1.54$ Å) radiation on a Philips XPert MPD apparatus.

The residual stress level was calculated from curvature measurements on thin specimens following coating deposition. The thin specimens were 25CD4 (0.25% carbon, 1% chromium) steel plates (80 mm × 18 mm × 1.5 mm). The curvature of the coated sample indicates both the sign and the level of residual stress [20].

Abrasion resistance tests were carried out with the abrasive tester described in Fig. 1. This method corresponds to the standard ASTM B 611-85 test method. A C20 (0.2% carbon) steel wheel with diameter of 179 mm and width of 16 mm is rotated in a slurry at 100 rev min^{-1}; four curved vanes are fixed to both sides of the wheel in order to stir and mix the abrasive slurry and to propel it towards the specimen during the test. The specimen is placed at the contact of the wheel, the pressure being applied by a load placed at the extremity of a lever. In the present work, the normal load on the specimen was fixed at 40 N. Alumina grits of different average grain size, 100 μm, 60 μm and 3 μm, were used. For each test, the abrasive was mixed with water in a water/abrasive weight ratio of 1:4. The specimen weight

Table 1
Spraying conditions

	APS1	APS2	VPS	CDS
Gun	PTF4	PTF4	PTF4	CDS100
Pressure (mbar)	1000	1000	30	1000
Ar flow rate ($l\,min^{-1}$)	47.5	47.5	50	
H_2 flow rate ($l\,min^{-1}$)	0	0	3	
He flow rate ($l\,min^{-1}$)	170	170	20	
Current (A)	700	700	730	
O_2 flow rate ($l\,min^{-1}$)				420
C_3H_8 flow rate ($l\,min^{-1}$)				60
Powder feed rate ($g\,min^{-1}$)	40	8 (for preheating) 40 (for spraying)	40	40
Carrier gas flow rate ($l\,min^{-1}$)	4	4	3	20
Spraying distance (mm)	125	125	375	300
Air cooling	Yes	Yes	No	Yes
Preheating	No	Yes	Yes	Yes
Injector diameter (mm)	1.8	1.8	3	2
Injection angle (°)	75	75	90	0
Nozzle diameter (mm)	6	6	6	8

Table 2
Spray powders

	Reference	Composition	Size distribution (μm)
APS and VPS	Amdry 983	WC–17% Co	<63
CDS	Amdry 1983	WC–17% Co	$+11$–45

loss was measured with a precision of 0.1 mg. Every 250 wheel revolutions, the test was interrupted to observe the coating surface and to weigh the specimen. The test was run until the coating was worn through. After these tests, worn surfaces were also examined by scanning electron microscopy (SEM).

3. Results and discussion

Optical micrographs of cross-sections of the layers deposited with the various process conditions are shown in Fig. 2. Dense WC–Co coatings were obtained with all processes. On the micrographs, the lighter grey corresponds to the cobalt-rich matrix. The fine, darker grey corresponds to the WC particles which are homogeneously distributed in the coatings and the darkest spots are pores.

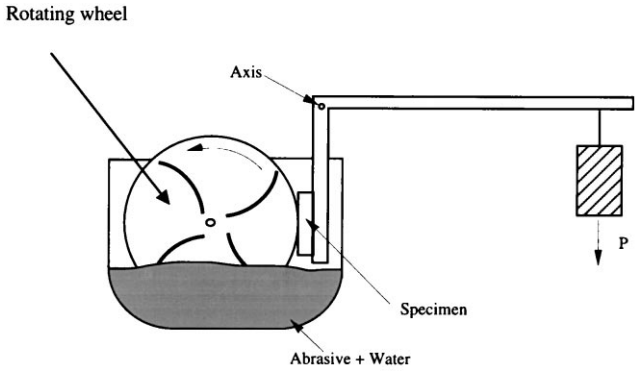

Fig. 1. Principle of the abrasive test device.

Traces of η-phase can be identified on the powder diffractogram, the presence of which results from the sintering step during fabrication [Figs. 3(a) and (e). In all cases the coatings present few mixed carbides (M_6C, $M_{12}C$) and W_2C [Figs. 3(b), (c), (d) and (f)]. Metallic cobalt is detected only in the coating obtained by the VPS process [Fig. 3(b)].

In accordance with observations previously cited, the X-ray patterns show a broad maximum in the range $2\theta = 38$ to 46° which is characteristic of the nanocrystalline or amorphous phases present in the coatings obtained by the APS 1 and 2 and CDS processes [Figs. 3(c), (d) and (f)].

Table 3 summarizes the coatings' characteristics in terms of microhardness, porosity and residual stresses.

The coating obtained with the CDS process exhibits the highest microhardness and the lowest rate of porosity. Corresponding values obtained with the other processes are almost identical between themselves.

The major difference between these coatings appears in the stress level. The sign of the global residual stress is positive for APS coatings and negative for VPS and CDS coatings, corresponding to a tensile and a compressive stress state, respectively. This behaviour can be related first to the thermal expansion coefficient of the substrate, which is higher than that of the coating, and

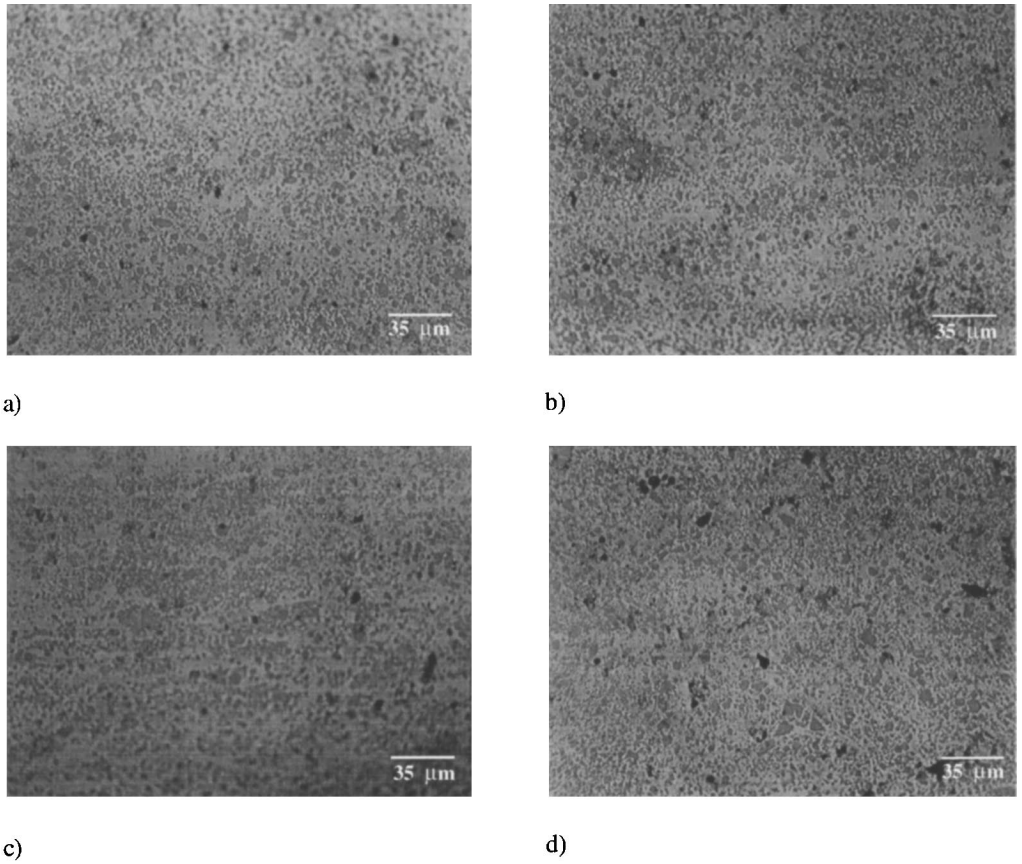

Fig. 2. Microstructure of the different coatings: (a) specimen APS1; (b) specimen APS1; (c) specimen CDS; (d) specimen VPS.

second to the fact that, in CDS and VPS conditions, the substrate temperature is higher and more homogeneous than in APS conditions; then the thermal spraying process creates compressive stresses during the cooling step of the sample. For APS2 the residual stress level is lower than in APS1 because the preheating stage used in the APS2 process reduces the thermal mismatch [20].

Weight losses versus the abrasive grain size resulting

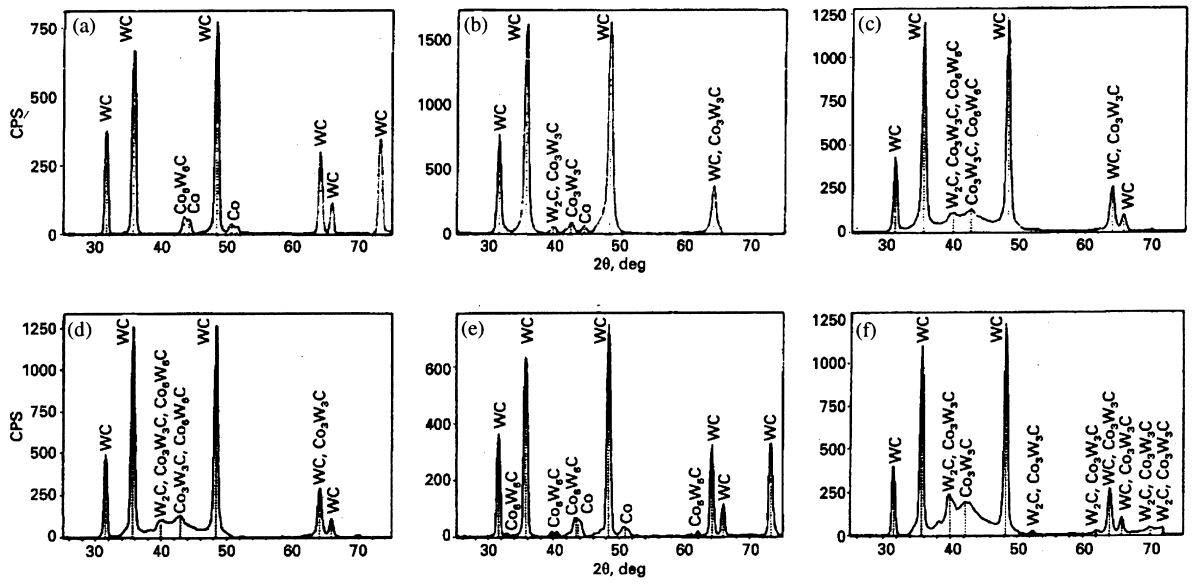

Fig. 3. XRD spectra of the WC–Co powders and as-sprayed coatings: (a) Amdry 983 powder; (b) VPS coating; (c) APS1 coating; (d) APS2 coating; (e) Amdry 1983 powder; (f) HVOF coating.

Table 3
Characteristics of the coatings

	APS1	APS2	VPS	CDS
Hardness ($HV_{0,3}$)	985(±26)	994(±32)	1096(±45)	1126(±30)
Macroporosity (%)	1.1(±0.5)	1(±0.5)	3(±1)	0.6(±0.1)
Internal stress (MPa)	+500(±25)	+200(±15)	−320(±17)	−180(±12)

from the abrasive test after 500 revolutions of the wheel are presented in Fig. 4. For the 3 μm average grain size abrasive, there is no difference in the weight losses of the different samples. With the 60 μm abrasive, a little difference can be noted between APS1, APS2 and CDS coatings, and already a large difference for the VPS coating. For the 100 μm abrasive, weight losses decrease for CDS and APS2 with respect to the situation with 60 μm abrasive while for the other processes they increase notably.

Globally, the weight loss of the specimen sprayed in VPS is always the highest, while that of the specimen sprayed with CDS is always the lowest. The weight loss of the APS2 specimen is close to that of the HVOF specimen, while the weight loss of the APS1 specimen is clearly higher.

Figs. 5 to 12 show the wear track morphologies for the different test conditions after 500 revolutions of the wheel.

For the uncoated specimen (Fig. 5) submitted to the abrasive with 100 μm grain size, the surface roughness is very high and presents micro-cutting and micro-ploughing tracks. The ratio of micro-cutting to micro-ploughing is related to the abrasive attack angle on the specimen surface. In the present case, the shape of the abrasive is rather irregular and consequently the attack angle is also irregular. Traces of micro-ploughing are very deep and abrasive particles embedded in the substrate can also be observed.

Under the same conditions, the wear morphology of the CDS coating presented in Fig. 6 is very different: in

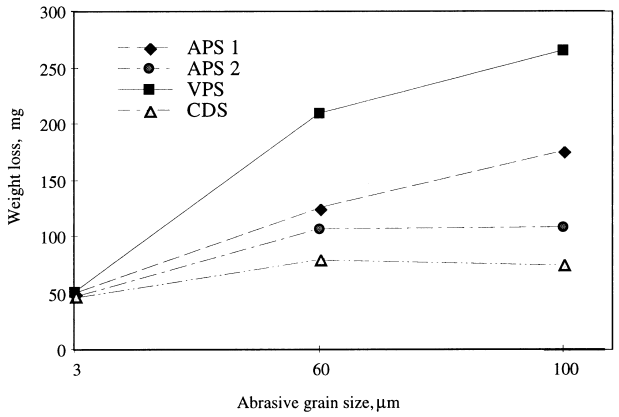

Fig. 4. Weight losses (±10 mg) of the different samples after 500 revolutions of the wheel versus the abrasive grain size.

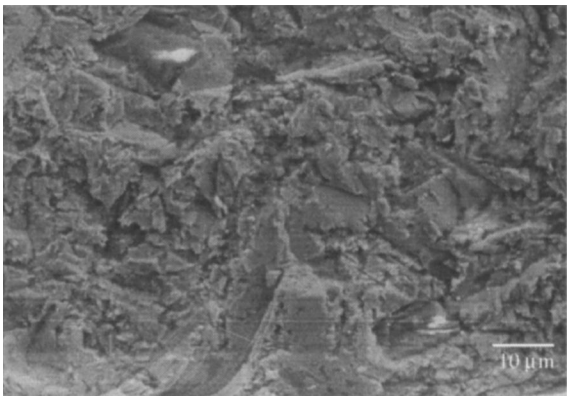

Fig. 5. Surface morphology of the steel substrate after 500 revolutions with the 100 μm abrasive.

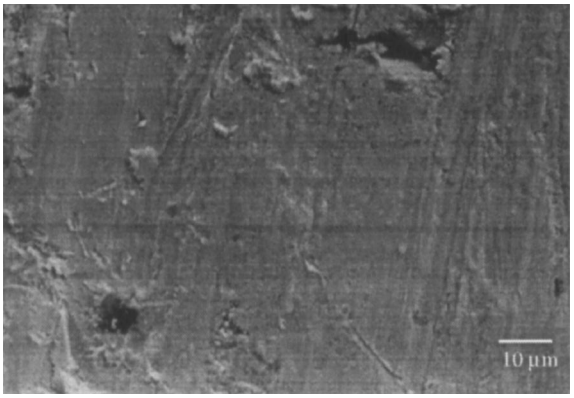

Fig. 6. Surface morphology of the CDS coating after 500 revolutions with the 100 μm abrasive.

Fig. 7. Surface morphology of the APS1 coating after 500 revolutions with the 100 μm abrasive.

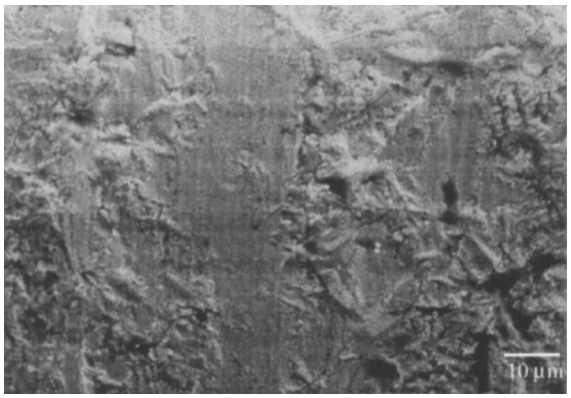

Fig. 8. Surface morphology of the APS2 coating after 500 revolutions with the 100 μm abrasive.

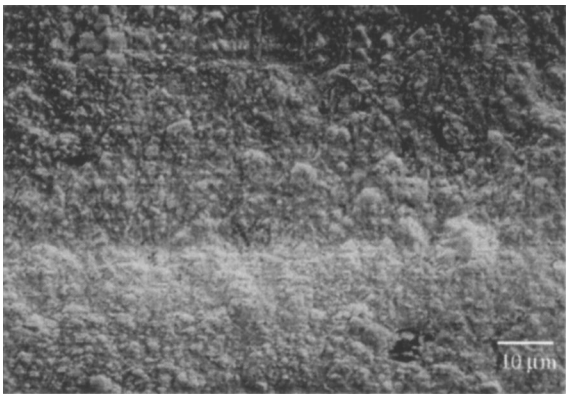

Fig. 11. Surface morphology of the CDS coating after 500 revolutions with the 3 μm abrasive.

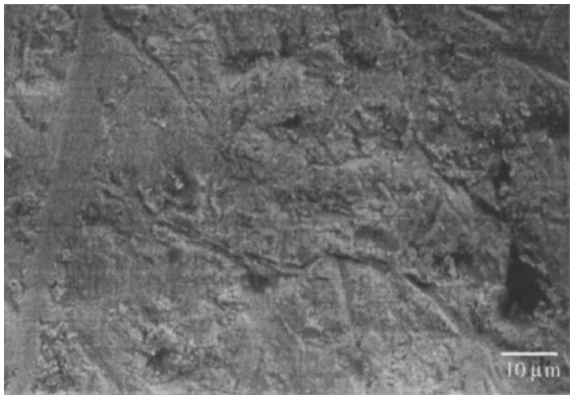

Fig. 9. Surface morphology of the VPS coating after 500 revolutions with the 100 μm abrasive.

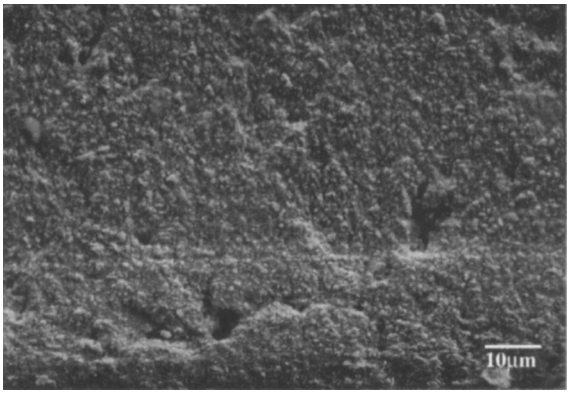

Fig. 12. Surface morphology of the VPS coating after 500 revolutions with the 3 μm abrasive.

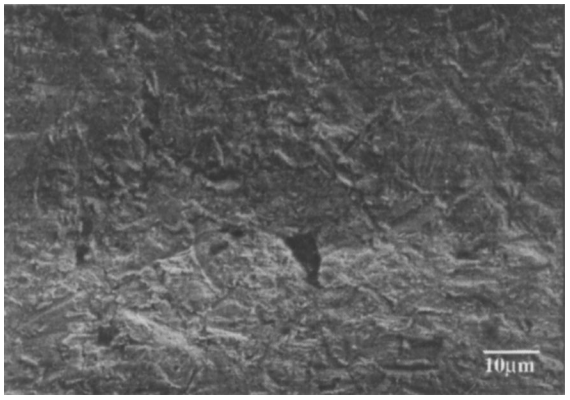

Fig. 10. Surface morphology of the CDS coating after 500 revolutions with the 60 μm abrasive.

this case, the major damage mechanism of the coating is micro-cutting and the surface remains rather smooth.

The other processes (Figs. 7–9) give similar wear morphologies, showing a mixture of micro-cutting and micro-ploughing but more pronounced than in the case of the CDS coating. Although the material is quite hard, some plastic deformation traces may be observed.

For the 60 μm abrasive (Fig. 10), micro-cutting and micro-ploughing are observed as well as some pull-out of carbide particles.

Figs. 11 and 12 show clearly the effect of particle size on the wear morphology. The small abrasive particles preferentially wear the matrix around WC particles, the toughness of the matrix favouring micro-cutting. This induces a periodicity in the surface roughness. When the matrix has been removed around the carbide particles, the latter are pulled out and holes appear on the surface. Thus, the smaller the abrasive particle size, the higher the wear resistance of these coatings, the hard carbide particles presenting a strong resistance when they are large enough compared with the abrasive particles. The 100 μm and 60 μm abrasive grains are larger than the carbide particles and so the abrasive particles cut or plough the coating, breaking carbide particles or pulling them out.

The effect of carbides on wear prevention thus depends on their quantity, morphology and distribution. When the size of the carbides particles is smaller than the wear track, carbides are too small to resist to the abrasive. Meanwhile, another important element for the abrasion resistance of cermets is the bond strength between the hard particles and the matrix. The higher

the link between the matrix and the particles, the better the resistance to abrasive wear will be.

XRD results show that the wear performance of the coatings is related to the presence of nanocrystalline structure observed in the APS and CDS coatings. This microstructure transformation identified, corresponding to diffusion following partial oxidation to form the mixed subcarbide, leads to an improvement of the binding between the hard particles and the matrix. In accordance with this analysis, the coating obtained by the VPS process presents the lowest abrasive wear resistance due to the lack of interaction between the phases.

Thus, the combination of the nanocrystalline microstructure and the η-phase has a favourable effect on the particle/matrix cohesion and therefore is helpful for the abrasion resistance of WC/Co coatings, even if the corresponding phases have a brittle behaviour.

Concerning the APS coating, it is observed that the abrasion resistance of APS2 is always better than that of APS1; this is understandable from the point of view of the mechanical solicitation of the surface during abrasion, the tensile stresses in APS2 being significantly lower than in APS1.

For the small (3 μm) abrasive particles, at first they remove the matrix around the carbide particles and do not really interact with the much bigger carbide particles. In this case, to resist abrasion, it is necessary to have a tough matrix rather than strong adhesion of the carbide particles to the matrix. Therefore, in this case, the behaviour of the VPS coatings is not different from the other ones.

4. Conclusion

In this work, the abrasive wear resistance of thermally sprayed WC–Co coatings was studied as a function of the thermal spray process and the grain size of the abrasive particles. Observations of the worn surface and XRD analyses permitted us to illustrate the relationship between microstructural transformations and the sample weight loss.

For resistance to abrasive wear, it is clear that the hardness and cohesion of the material are very important, especially for cermets like WC/Co. In these materials the hard WC particles increase the mean hardness and the cobalt matrix acts as a binder which links the carbide particles and increases the material toughness. Thus, in order to increase the abrasion resistance of this material, it is very important to increase the cohesion between the carbide particles and the cobalt matrix; this cohesion is related to the amorphous or nanocrystalline interaction phases in the coatings at the interface between the carbides and the matrix.

The appearance of M_6C or $M_{12}C$ carbides in thus an indication of the level of interaction between tungsten carbide particles and the matrix, which results in an increase of the cohesion and consequently in an improvement of the abrasion resistance.

From the abrasion test results it appears that the smaller the abrasive size, the better a coating's resistance to abrasive wear whatever its microstructure. But when the grain size of the abrasive is larger than the tungsten carbide particles, the role of the coating process, which conditions the coating structure, is emphasized, and the HVOF process gives the better abrasion resistance. In this case, as well as the matrix (toughness, low porosity) and carbide properties (hardness, brittleness), the tungsten carbide–matrix interactions seems to play a major role in the cohesion of the structure and therefore in its abrasion resistance.

Residual stresses also have an influence on the resistance to abrasive wear because they interact with the mechanical solicitation of the surface. In this respect, tensile stresses are unfavourable to the abrasion resistance. Specific control of spraying conditions was shown to reduce the stress level significantly and thus to increase the abrasive wear resistance of thermally sprayed WC/Co coatings.

References

[1] C. Chuanxian, H. Bingtain, L. Huiling, Plasma wear resistance of ceramic and cermet coating materials, Thin Solid Films 118 (1984) 485–493.
[2] A. Karimi, C. Verdon, G. Barbezat, Microstructure and hydroabrasive wear behaviour of high velocity oxy-fuel thermally sprayed WC–Co–(Cr) coatings, Surf. Coat. Technol. 57 (1993) 81–89.
[3] K.-H. Zum Gahr, Microstructure and Wear of Materials, Elsevier Science Publishers BV, Amsterdam, 1987.
[4] A.R. Nicoll, A. Bachmann, J.R. Moens, G. Loewe, The application of high velocity combustion spraying, in: C.C. Berndt (Ed.), Thermal Spray International Advance in Coatings Technology, ASM International, Metals Park, OH, 1992, pp. 149–152.
[5] S.F. Wayne, S. Sampath, Structure/property relationship in sintered and thermally sprayed WC/Co, J. Therm. Spray Technol. 1 (4) (1992) 304–307.
[6] Y. Wang, P. Kettunen, The optimization of spraying parameters for WC–Co coatings by plasma and detonation-gun spraying, in: C.C. Berndt (Ed.), Thermal Spray International Advances in Coatings Technology, ASM International, Metals Park, OH, 1992, pp. 575–580.
[7] J. Nerz, B. Kushner, A. Rotolico, Microstructural evaluation of tungsten carbide–cobalt coatings, J. Therm. Spray Technol. 1 (2) (1992) 147–152.
[8] B. Arsenault, J.-P. Immarigeon, V.R. Paramweswaran, H. Hawthorne, J.G. Legoux, Slurry and dry erosion of high velocity oxy-fuel thermal spray coatings, in: C. Coddet (Ed.), Thermal Spray: Meeting the Challenges of the 21st Century vol. 1, ASM International, Metals Park, OH, 1998, pp. 231–236.
[9] B. Schultrich, L.M. Berger, J. Menker, A. Oswald, Influence of carbide powder composition on decarburization during air plasma spraying, in: H. Eschnauer (Ed.), Proceedings of 2nd Plasma-Technik Symposium, Lucerne, Switzerland vol. 2 (1991) 363–371.